

Inner-shell excitations and ionizations of atomic ions by high-energy electron impact

Yukap Hahn

Department of Physics, University of Connecticut, Storrs, Connecticut 06268
(Received 10 October 1975; revised manuscript received 1 December 1975)

Cross sections for the inner-shell ionization of argon ions by high-energy electron impact are estimated. An improved form of the single-particle model with varying degrees of ionization is used in the calculation of the excitation amplitudes. Partial sums over the allowed final states are carried out using the semiclassical projection operator. This operator depends on a spectral cutoff parameter e_b , and a method for its determination is examined for the case of hydrogenic transitions. The ionization cross section incorporates both the direct excitation to the continuum and the Auger emission following the inner-shell excitations. For electron energies in the KeV range and for atomic targets with the core charges Z_C less than 20, the direct ionization dominates, with the excitation Auger-emission mode making a small but appreciable contribution. The ionization cross sections for the neutral neon, and oxygen targets are also estimated.

I. INTRODUCTION

In a previous study¹ of the electron-impact ionization of ionic targets, we estimated the relevant excitation probabilities for the target ions with the core charges Z_C in the range $10 \lesssim Z_C \lesssim 80$ and the degree of ionization Z_I in the range $0 \lesssim Z_I \lesssim Z_C$. In the case of neutral atoms, with $Z_I=0$, the system was represented by the single-particle model obtained earlier phenomenologically by Green *et al.*² On the other hand, for targets which are initially ionized to the degree Z_I , we made an *ad hoc* extension of the model by adjusting one of the parameters which appear in the model. Such a crude extension was nevertheless sufficient in a preliminary study carried out in Ref. 1.

More recently, however, Szydlik and Green³ re-examined the extended model for $Z_I \neq 0$ and found that the screening part of the earlier potential did not decay fast enough and consequently gave excessive bindings. The variation of the parameter (d) as a function of Z_I for each fixed Z_C shows rather complicated features. We adopt here the new parametrization³ and examine its effect on the ionization cross section.

The inner-shell excitations by high-energy-electron impact either to higher bound-state configurations or to the continuum requires a restricted sum over all of the allowed single-electron states. This *partial sum* can be conveniently carried out⁴ in terms of the semiclassical projection operator Λ , and construction of such operators is facilitated by the use of the simple local single-particle potential. Thus one of the bound-state electrons can be ionized by directly promoting it to the continuum or by first exciting it to a higher unoccupied state followed by an Auger-electron emis-

sion; the vacancy can also be filled by an electron with the emission of a photon, and this branching ratio is available in terms of the fluorescence yield.⁵

We consider in this paper specifically reactions involving the argon target with varying degrees of ionization Z_I . The theoretical method employed here¹ is applicable to other atomic targets as well, once an improved model potential is available. The semiclassical projection operator is especially simple to use when the single-particle states are generated by a local potential, and allows one in a simple way to approximately sum a part of the complete spectrum of a one-particle system. To further clarify the effectiveness and reliability of the approach adopted here for the estimate of the electron-impact ionization cross section, we will also present the result for the neutral neon and oxygen targets, which can be compared with the existing theoretical and experimental results.

II. THEORY

The theory of electron-impact ionization of target atoms is rather well known,^{6,7} and an approximate procedure to estimate its cross section was described previously.¹ Therefore we review here briefly only those parts of the formalism which are relevant to the present discussion and in defining notation. The electron-atom inelastic excitation cross section for the transition $\alpha \rightarrow \beta$ is given at high energies by

$$I_{\alpha\beta}(\theta) = \left(\frac{m}{2\pi\hbar^2} \right)^2 \frac{k_\beta}{k_\alpha} Z_\alpha \times \left| \int \int d^3r d^3R \psi_\beta^*(\vec{r}) \mathbf{V}_s \psi_\alpha(\vec{r}) e^{i\vec{q} \cdot \vec{R}} \right|^2, \quad (2.1)$$

where \vec{r} denotes collectively the internal target-electron coordinates and \vec{R} is the scattering electron with momentum \vec{k}_α or \vec{k}_β . The electron being scattered is described in (2.1) by plane wave without distortions; \vec{q} denotes the momentum transfer, $\vec{q} = \vec{k}_\alpha - \vec{k}_\beta$. The target states are described by ψ_α and ψ_β with the energies e_α and e_β , while the interaction between the target electron and the projectile is given by $V_S = e^2/|\vec{r}_S - \vec{R}|$. The number of electrons in the α th subshell is represented by Z_α . In terms of the Bethe integral⁸ in the dipole approximation, we have, with $m = \hbar = e^2 = 1$,

$$I_{\alpha\beta}(\theta) \approx (k_\beta/k_\alpha) Z_\alpha (4/q^2) \bar{M}_{\beta\alpha}, \quad (2.2)$$

where

$$\bar{M}_{\beta\alpha} \equiv \left| \int d^3r \psi_\beta(\vec{r}) \vec{n} \cdot \vec{r}_S \psi_\alpha(\vec{r}) \right|^2, \quad (2.3)$$

with $\vec{q} \equiv \vec{n}q$. After integration over the scattering angles, the total cross section is given by

$$\sigma_{\alpha\beta}(k_\alpha) = (8\pi Z_\alpha/k_\alpha^2) \bar{M}_{\beta\alpha} \ln(q_{\max}/q_{\min}), \quad (2.4)$$

where obviously

$$q_{\max} = k_\alpha + k_\beta, \quad q_{\min} = k_\alpha - k_\beta. \quad (2.5)$$

Depending on the choice of k_β , q_{\max} and q_{\min} will change; from energy conservation, we have

$$k_\alpha^2 = k_\beta^2 - 2m(e_\alpha - e_\beta)/\hbar^2. \quad (2.6)$$

We now consider several ways by which q_{\max} and q_{\min} may be approximated.⁸ For high-energy scattering with $E_k \gg |e_\alpha|$, we may set

$$q_{\min} \approx m(e_\beta - e_\alpha)/\hbar^2 k_\alpha \equiv m\Delta_{\alpha\beta}/\hbar^2 k_\alpha. \quad (2.7)$$

On the other hand, the q_{\max} may take different forms depending on the physical picture one introduces. For example, we may set $q_{\max} \approx 2k_\alpha$, which is mathematically consistent with (2.5) and (2.6), with the result

$$\ln(q_{\max}/q_{\min}) \approx \ln(4E_\alpha/\Delta_{\alpha\beta}). \quad (2.7a)$$

However, this is not quite correct from the physical point of view; the high-energy scattering from a weakly bound system will take place mainly within the first diffraction peak, i.e., for $q \lesssim 3.832r_\alpha^{-1}$, where the numerical factor is the first zero of the Bessel function J_1 and r_α is roughly the size of the scatterer electron, with $r_\alpha^{-1} \approx (2|e_\alpha|)^{1/2}$. In fact the Bethe approximation and the dipole approximation $qr_\alpha \ll 1$ introduced in the derivation of (2.2) are consistent with the above picture. Thus with $q_{\max} \approx r_\alpha^{-1} \approx (2|e_\alpha|)^{1/2}$ we obtain the usual result,

$$\ln(q_{\max}/q_{\min}) \approx \frac{1}{2} \ln(4E_\alpha/\Delta_{\alpha\beta}), \quad (2.7b)$$

which is a factor of 2 smaller than (2.7a). In the following, we adopt the form (2.7b), keeping in mind the above uncertainty. Therefore we have

$$\sigma_{\alpha\beta}(k_\alpha) \approx (4\pi Z_\alpha/k_\alpha^2) \bar{M}_{\beta\alpha} \ln(4E_\alpha/\Delta_{\alpha\beta}). \quad (2.8)$$

The sum over the final allowed states β gives, for β in the bound and continuum configurations which are not occupied,

$$\begin{aligned} \sigma_\alpha^A &\equiv \sum'_{\beta \in B, C} \sigma_{\alpha\beta}^A \\ &\approx (\pi a_0^2) \frac{4Z_\alpha}{(k_\alpha a_0)^2} \ln\left(\frac{4E_\alpha}{\Delta_\alpha^D}\right) \bar{M}_E^\alpha W_\alpha, \end{aligned} \quad (2.9)$$

where

$$\bar{M}_E^\alpha \equiv [1/3(2l+1)][(l+1)M_E^{n_l^+} + lM_E^{n_l^-}], \quad (2.10)$$

with n_l for the particular initial configuration α , $l_\pm \equiv l \pm 1$ and

$$M_E^{n_l^\pm} \equiv M_E^\alpha = \sum_\beta M_{\beta\alpha}. \quad (2.11)$$

($M_{\beta\alpha}$ is the radial part of $\bar{M}_{\beta\alpha}$, and the angular part is included in \bar{M}_E^α .) The subscript E implies that the set includes all the allowed excited states of the target, including the continuum. In (2.9) we have added the Auger branching ratio W_α , which is estimated from the known fluorescence yield⁵ Y_α by $W_\alpha = 1 - Y_\alpha$. Similarly, we have for the direct ionization

$$\sigma_\alpha^C \approx (\pi a_0^2) [4Z_\alpha/(k_\alpha a_0)^2] \ln(4E_\alpha/\Delta_\alpha^C) \bar{M}_C^\alpha, \quad (2.12)$$

where $M_C^{n_l^\pm}$ and \bar{M}_C^α are defined in a manner similar to (2.10) and (2.11).

Finally, the total cross section is obtained by summing over all the *occupied* bound-state configurations,

$$\sigma^A(Z_C, Z_I, E) = \sum_\alpha \sigma_\alpha^A, \quad (2.13)$$

$$\sigma^C(Z_C, Z_I, E) = \sum_\alpha \sigma_\alpha^C. \quad (2.14)$$

Incidentally, the excited states of the target may also decay by the radiation emission rather than by the Auger-electron emission. Its cross section σ^R is then given immediately by

$$\sigma^R(Z_C, Z_I, E) = \sum_\alpha \sigma_\alpha^R, \quad (2.15)$$

where

$$\sigma_\alpha^R \approx (\pi a_0^2) [4Z_\alpha/(k_\alpha a_0)^2] \bar{M}_E^\alpha (1 - W_\alpha) \ln(4E_\alpha/\Delta_\alpha^D). \quad (2.16)$$

III. SINGLE-PARTICLE MODEL AND INNER-SHELL EXCITATION PROBABILITIES

For the bare-core nuclear charge $Z_C = 18$ for Ar and the degree of ionization Z_I (with $Z_I = 0$ for a neutral atom), we have the single-particle-

model potential^{2, 3} given by

$$V(r) = (e^2/r)[(Z_C - Z_I - 1)U(r) - Z_C], \quad (3.1)$$

where

$$U(r) = 1 - \Omega(r), \quad (3.2)$$

$$\Omega(r) = [H(e^{r/d} - 1) + 1]^{-1}. \quad (3.3)$$

In (3.3), we have two parameters d and H , which are determined by Green *et al.*³; the values used here for Ar are listed in Table I for various degrees of ionization. The Z_I dependence of the parameter d , which was neglected in the previous study,¹ has a dramatic effect on the binding energies. The parameter H , or $K = H/d$, also depends on Z_I with appreciable improvement in the binding energies.

The radial part of the excitation probabilities M_E^α and M_C^α defined by (2.14) and (2.16) is estimated using the projection operator Λ_E^α and Λ_C^α to be specified below.¹ If the highest occupied state of given $l_\pm = l \pm 1$ has the energy $e_{n_g l_\pm}$ and the lowest unoccupied state has the energy $e_{n_0 l_\pm}$, then the unoccupied bound-state projection for all the states above e_b and below the ionization threshold is given by⁴

$$\begin{aligned} \Lambda_D^{l_\pm}(r, r') &= \frac{1}{\pi r r' u} \sin(P_b u) \\ &\approx \sum_{n'' \geq n_0} R_{n''}^{l_\pm}(r) R_{n''}^{l_\pm}(r'), \end{aligned} \quad (3.4)$$

where

$$\begin{aligned} u &\equiv |r - r'|, \quad \psi_{n'' l_\pm}(\vec{r}) = R_{n''}^{l_\pm}(r) Y_{l_\pm}^m(\Omega_r), \\ P_b &= P_b(v) = [2e_b - 2V(v) - L_\pm^2 v^{-2}]^{1/2} \end{aligned} \quad (3.5)$$

with

$$v \equiv \frac{1}{2}(r + r'), \quad L_\pm = (l_\pm + \frac{1}{2})^2.$$

The spectrum projected by $\Lambda_D^{l_\pm}$ is therefore cut off from below by the parameter e_b , which is related to the energy of the lowest unoccupied excited state $e_{n_0 l_\pm}$ by $e_{n_0 l_\pm} \geq e_b$, and from above by

the ionization threshold $e_{n_l} = 0$. The range of integrations over the variables r and r' involved in Λ is such that P_b of (3.5) remains real and positive, in accordance with the classical picture adopted in the construction of Λ . The projection operators which are needed in M_E^α and M_C^α are then given by

$$\Lambda_C^\alpha = \delta(r - r') - \Lambda_B^\alpha, \quad \Lambda_B^\alpha \equiv \Lambda_D^\alpha(e_b \rightarrow -\infty) \quad (3.6)$$

and

$$\Lambda_E^\alpha = \Lambda_C^\alpha + \Lambda_D^\alpha, \quad (3.7)$$

where Λ_B^α in (3.6) projects onto *all* of the bound-state configurations, both filled and unfilled, while Λ_D^α spans only over the allowed unoccupied configurations. Thus, the relation (3.6) is a direct consequence of the closure property, while Λ_E^α in (3.7) excludes those states which lie below the cutoff energy e_{n_0} . The transition probabilities for $(n, l) \rightarrow (\text{continuum}, l_\pm)$ and $(n, l) \rightarrow (\text{all allowed states})$ are given respectively by

$$\begin{aligned} M_C^\alpha &= M_C^{n l_\pm} = \langle n l | r^2 | n l \rangle - \langle n l | r \Lambda_B^{n l_\pm} r' | n l \rangle \\ &\equiv M_A^\alpha - M_B^\alpha \end{aligned} \quad (3.8)$$

and

$$M_E^\alpha = M_E^{n l_\pm} = \langle n l | r \Lambda_E^{n l_\pm} r' | n l \rangle = M_C^\alpha + M_D^\alpha. \quad (3.9)$$

For test purposes, we may also define the overlap integral S_{nl} , which should be 1 or 0 for $n \geq n_0$ or $n < n_0$, respectively, as

$$S_{nl} = \langle n l | \Lambda_B^{l_\pm} | n l \rangle. \quad (3.10)$$

As noted earlier, M_D^α and M_E^α depend on the cutoff parameter e_b when any of the low-lying l_\pm shells are occupied. (Note that M_A , M_B , and M_C do not depend on e_b .) To examine this dependence, we have first estimated M_D^α for the case of hydrogen ($Z_C = 1$, $Z_I = 0$) with $\alpha \equiv (n, l) = (1, 0)$, $(2, 0)$, and $(2, 1)$, for which the exact result is available⁹ for comparison. The transition probabilities are calculated as functions of $|e_b| \equiv n_b^{-2}$ for the transitions

TABLE I. Single-particle energy e_{nl} of the argon ion calculated using the potential (3.1) and the parameters d and H . The single-particle energies are given in rydbergs. Z_I denotes the degree of ionization, with $Z_I = 0$ for the neutral Ar atom. The last column contains the correct ionization energies. The ionization energies are given in Refs. 21 and 22, while the values for d and H are from Ref. 3.

Z_I	d	K	H	1s	2s	2p	3s	3p	Ionization energy
16	0.042	20.1	0.843	302.2					320
14	0.090	9.55	0.863	282.4	61.86				63
8	0.180	5.62	1.012	242.7	35.10	30.66			31
6	0.274	4.98	1.37	236.9	30.26	25.87	8.86		9.4
0	1.045	3.50	3.66	228.0	21.67	17.35	1.91	1.21	1.16

$$(n, l) \rightarrow \sum_{n''} (n'' \geq n_0, l \pm 1),$$

where n'' covers all the allowed states above n_b . The calculated result is summarized in Figs. 1–3 which indicate the general trend of the shift in the correct e_b for different n_0 . That is, for $n_0 \leq 4$ we have $n_b \approx n_0 - \frac{1}{2}$, while for $n_0 \geq 4$ we have to choose $n_b \approx n_0 - 1$. It seems difficult to choose the correct value for e_b very accurately, and this will be reflected in the error estimate in the final M_E^α and M_D^α .

The above feature of e_b being dependent on the value of n_0 for different Z_C and Z_I has been incorporated in the actual estimate of M_D^α and M_E^α for the argon case, and the result is summarized in Table II. The transition probabilities M_D^α increase markedly as we go to outer shells.

In connection with the determination of the cutoff energy, it is also important to estimate the value for the e_b in the limit $n \rightarrow \infty$. The position

$$e_c \equiv \lim_{n \rightarrow \infty} e_b$$

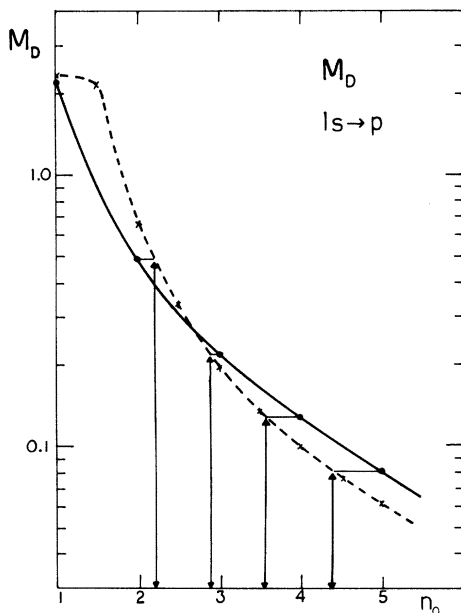


FIG. 1. Radial part of the dipole transition probability $M_D^{1/2}$ for the hydrogenic system, $Z_C=1$ and $Z_I=0$, and $(n, l) = (1, 0) \rightarrow (n', l') = (n', 1)$. $M_D^{1/2}$ depends on the cutoff parameter e_b , or rather on $n_b \equiv (e_b)^{-1/2}$. The dashed curve is obtained using the semiclassical operator Λ_D , while the solid curve is the exact result. The arrows indicate the correct values of n_b for which Λ_D gives the correct M_D . For example, to include all of the states with $n' \geq 2$ requires $n_b \approx 1$, to include all of the states with $n' \geq 3$ requires $n_b \approx 2.2$, and so on. Note that, approximately, $n_0 \approx n_b + 1$, where n_0 denotes the principal quantum number for the lowest unoccupied state to be included in Λ_D .

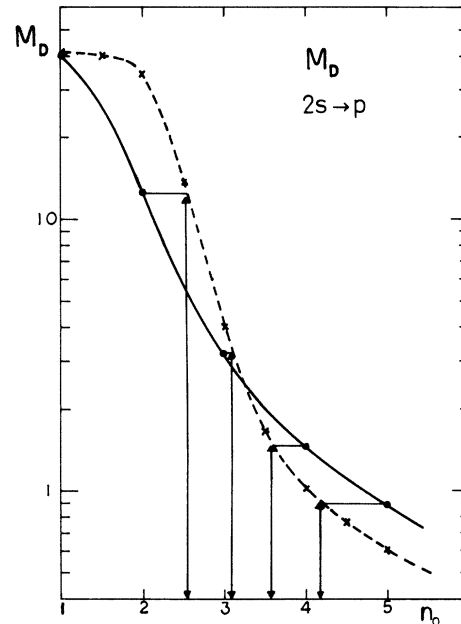


FIG. 2. Radial part of the dipole transition probability $M_D^{1/2}$ for the hydrogenic system, $Z_C=1$ and $Z_I=0$, and $(n, l) = (2, 0) \rightarrow (n', l') = (n', 1)$. The dashed curve is obtained with Λ_D (semiclassical) and the solid curve is the exact result.

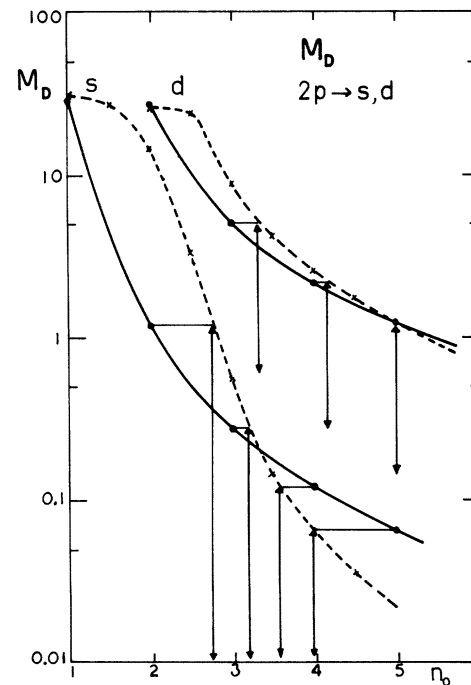


FIG. 3. Radial part of the dipole transition probability $M_D^{1/2}$ for the hydrogenic system, with $(n, l) = (2, 1) \rightarrow (n', 0)$ or $(n', 2)$. The dashed curves are the semiclassical result and the solid curves are exact.

should be important sometimes in the calculation of M_C and M_D . The values for M given in Table II are obtained with $e_c=0$, except the case for the last row with $Z_I=0$, and $nl=3p-d$. We have seen from Figs. 1–3 that, as n increases, n' lags behind more, and the limit point for n' may not be at infinity. In fact, we can roughly estimate that n' may somewhere approach $n' \gtrsim 10$ as $n \rightarrow \infty$, giving $Z e_c \cong -Z^2/(10)^2$. This value will be used later to correct for M_C . The last row in Table II is obtained with $e_c \cong -0.06$ Ry; note the change in M_C .

Incidentally, we note that within the dipole Bethe approximation of (2.3), these transition probabilities are independent of the scattering energy. The dependence of the cross sections σ_α^A and σ_α^C on the projectile energy E_α is entirely contained in the factor $E_\alpha^{-1} \ln(E_\alpha/\Delta_\alpha)$, so that the values given in Table II can be used for all energies E_α , so long as the underlying Born approximation in (2.1) is valid; this limits the applicability of the formalism of this section to high-energy-electron impact.

IV. ELECTRON-IMPACT IONIZATION CROSS SECTIONS

The excitation probabilities M for the various subshells obtained in Sec. III can now be used to

evaluate the ionization cross sections, both for the direct and excitation modes. Since the cross-section formula derived in Sec. II neglects the Coulomb distortions in the initial and final states of the scattering electron when $Z_I > 0$, we expect (2.3) to be effective for the initial energy $E_k \cong E_\alpha$ in the region where

$$|e_\alpha/E_\alpha| \ll 1; \quad (4.1)$$

that is, roughly, for the argon ion with $Z_C=18$,

$$E_k \gtrsim 10 \text{ keV} \quad (4.2)$$

for all Z_I and

$$E_k \gtrsim 1 \text{ keV} \quad (4.3)$$

for $Z_I \leq 14$ and $n \geq 2$. The E_k is also limited from above by

$$E_k \leq 100 \text{ keV} \quad (4.4)$$

as we also neglect the relativistic kinematic effect. (As in Ref. 1, the relativistic correction can be incorporated in a trivial way if necessary.)

Table III contains the calculated cross sections σ_α^A and σ_α^C at $E_k=10$ keV and for the different degrees of ionization Z_I . The multiplicity param-

TABLE II. Radial part of the dipole transition probabilities for $(nl) \rightarrow (n', l_\pm \equiv l \pm 1)$. S involves the overlap between ψ_{nl} and $\Lambda_{n'l}$. M_A is the total transition probability, and M_B is the total bound-state transitions, with the n' spanning all of the bound-state configurations; M_C is the total continuum-state transition probability, with the n' spanning all of the continuum states. Thus $M_A = M_B + M_C$. M_D selects only those bound-states which are unoccupied, as specified by the cutoff parameter e_b ; $M_E = M_D + M_C$. All M 's are given in atomic units. The case $e_b \equiv a$ implies no cutoff, thus $M_D = M_B$. The entry in the last row for $Z_I=0$ and $nl=3p$ is obtained with the threshold cutoff $e_c = -0.06$ Ry.

Z_I	nl	l_\pm	S	M_A	M_B	M_C	e_b (Ry)	M_D	M_E
16	1s	p	0.900	0.010	0.007	0.003	a	0.007	0.010
14	1s	p	0.900	0.010	0.007	0.003	a	0.007	0.010
	2s	p	0.939	0.156	0.152	0.005	a	0.152	0.156
8	1s	p	0.900	0.010	0.006	0.004	20.0	0.001	0.005
	2s	p	0.946	0.201	0.191	0.010	20.0	0.081	0.091
	2p	s	0.959	0.169	0.169	0.000	30.0	0.084	0.084
	2p	d	0.959	0.169	0.129	0.039	a	0.129	0.168
6	1s	p	0.898	0.010	0.006	0.004	20.0	0.001	0.004
	2s	p	0.937	0.205	0.191	0.014	20.0	0.123	0.137
	2p	s	0.952	0.172	0.172	0.000	6.0	0.002	0.002
	2p	d	0.952	0.172	0.118	0.054	a	0.118	0.172
	3s	p	0.963	1.66	1.64	0.024	20.0	1.64	1.67
0	1s	p	0.893	0.010	0.006	0.004	1.0	0.000	0.004
	2s	p	0.908	0.210	0.179	0.030	1.0	0.004	0.035
	2p	s	0.923	0.176	0.174	0.002	1.3	0.002	0.004
	2p	d	0.923	0.176	0.042	0.134	a	0.042	0.176
	3s	p	0.897	2.74	2.40	0.338	1.0	1.37	1.71
	3p	s	0.903	3.28	3.26	0.026	1.3	1.92	1.94
	3p	d	0.903	3.28	1.86	1.42	a	1.86	3.28
0	3p	d	0.903	3.28	1.62	1.66	a	1.62	3.28

TABLE III. Calculation of the direct ionization cross sections σ^C for the argon ions by the electron impact at $E_k = 10$ keV. The various parts in the formula (2.15) are shown explicitly. The numbers in parentheses denote the powers of 10 by which the terms preceding them are multiplied.

Z_I	nl	l_{\pm}	Z_{α}	\bar{M}_C^{α}	Δ_{α}^C (Ry)	$\sigma_{\alpha}^C(\pi a_0^2)$	$\sigma^C(\pi a_0^2)$
16	1s	p	2	0.0008	338	2.0 (-5)	2.0 (-5)
14	1s	p	2	0.0009	307	2.3 (-5)	2.3 (-5)
	2s	p	2	0.0015	87	5.8 (-5)	8.1 (-5)
8	1s	p	2	0.0013	248	3.4 (-5)	3.4 (-5)
	2s	p	2	0.0034	40	1.6 (-4)	1.9 (-4)
	2p	s, d	6	0.0085	36	1.2 (-4)	3.1 (-4)
6	1s	p	2	0.0013	240	3.6 (-5)	3.6 (-5)
	2s	p	2	0.0045	33	2.2 (-4)	2.6 (-4)
	2p	s, d	6	0.012	29	1.8 (-3)	2.1 (-3)
	3s	p	2	0.008	12	4.7 (-4)	2.6 (-4)
0	1s	p	2	0.0014	229	4.1 (-5)	4.1 (-5)
	2s	p	2	0.010	22	5.4 (-4)	5.8 (-4)
	2p	s, d	6	0.030	18	5.0 (-3)	5.6 (-3)
	3s	p	2	0.112	2.6	8.6 (-3)	1.4 (-2)
	3p	s, d	6	0.320	1.9	7.7 (-2)	9.1 (-2)
0	3p	s, d	6	0.320	1.9	8.9 (-2)	1.0 (-1)

eter Z_{α} for the subshell α is taken to be

$$Z_{\alpha} = 2(2l+1), \quad \alpha \equiv (n, l), \quad (4.5)$$

and the average excitation energy Δ_{α}^C is chosen to be approximately

$$\Delta_{\alpha}^C \approx \frac{1}{2} |e_{n_0} - e_{\alpha}|, \quad (4.6)$$

where e_{n_0} is the energy for the lowest unoccupied state for given Z_I . The drastic increase in the excitation cross sections to the continuum as we go to the higher shells comes mainly from the increase in \bar{M}_C^{α} , but the Δ_{α}^C -dependent factor also contributes significantly to this increase.

The excitation-ionization cross sections σ_{α}^A and σ^A are given in Table IV; we have chosen here

$$\Delta_{\alpha}^D \approx -\frac{1}{2} |e_{n_0} - e_{\alpha}| \quad \text{and} \quad \Delta_{\alpha}^E \approx |e_{\alpha}|, \quad (4.7)$$

rather than the choice (4.6). The additional factor W_{α} in σ_{α}^A for the Auger branching ratio is taken from Ref. 5. However, for the highest occupied shell for given Z_I , we have set $W_{\alpha} = 0$. This is entirely consistent with the physical picture of the Auger emission, as, by definition, there are no higher-shell electrons available to fill such states with enough energy released to eject electrons. (To be more precise, W_{α} is not strictly zero since we have at least two electrons in the higher shells, one electron promoted in the process of excitation and the other incoming electron when a large loss of energy is involved.) Thus, although the excitation probability is high for the outer electrons, such vacancies are filled by a radiative emission.

In Table V, we collect for the argon case the contributions from σ^C and σ^A to the total ionization cross section σ^I ; the effect of σ^A is not negligible, and, as we have seen in the earlier study,¹ σ^A in fact dominates for $Z_C \geq 40$.

TABLE IV. Calculation of the excitation ionization cross section σ^A for the argon ions by electron impact at $E_k = 10$ keV. The various parts in the formula (2.12) are shown explicitly. The Auger-emission branching ratio W_{α} is obtained from the fluorescence yield Y_{α} by $W_{\alpha} = 1 - Y_{\alpha}$. The numbers in the bracket denote the powers of 10 by which the terms preceding them are multiplied. The values for the fluorescence yield are from Ref. 5. The underlined values for σ^A are used in the estimate of the total ionization cross section σ^I .

Z_I	nl	l_{\pm}	Z_{α}	\bar{M}_E^{α}	Δ_{α}^E (Ry)	W_{α}	$\sigma_{\alpha}^A(\pi a_0^2)$	$\sigma^A(\pi a_0^2)$
16	1s	p	2	0.0032	302	0.84	6.7 (-5)	6.7 (-5)
14	1s	p	2	0.0033	282	0.84	7.0 (-5)	<u>7.0 (-5)</u>
	2s	p	2	0.053	62	1.00	2.2 (-3)	2.2 (-3)
8	1s	p	2	0.0015	243	0.84	3.5 (-5)	<u>3.5 (-5)</u>
	2s	p	2	0.030	35	1.00	1.5 (-3)	1.5 (-3)
	2p	s, d	6	0.047	31	1.00	7.0 (-3)	8.5 (-3)
6	1s	p	2	0.0014	237	0.84	3.3 (-5)	3.3 (-5)
	2s	p	2	0.044	30	1.00	2.2 (-3)	2.2 (-3)
	2p	s, d	6	0.038	26	1.00	6.1 (-3)	<u>8.3 (-3)</u>
	3s	p	2	0.008	8.9	1.00	4.7 (-4)	8.8 (-3)
0	1s	p	2	0.0014	228	0.84	3.4 (-5)	3.4 (-5)
	2s	p	2	0.012	22	1.00	6.2 (-4)	6.5 (-4)
	2p	s, d	6	0.040	17	1.00	6.8 (-3)	<u>7.5 (-3)</u>
	3s	p	2	0.57	1.9	1.00	4.6 (-2)	5.4 (-2)
	3p	s, d	6	0.94	1.2	1.00	2.4 (-1)	2.9 (-1)

TABLE V. Total ionization cross section $\sigma^I = \sigma^C + \sigma^A$ for the argon ions of ionization degree Z_I and the electron-impact energy $E_k = 10$ keV. σ^R is the radiation emission cross section for the Ar ion after it is excited. All cross sections are given in the πa_0^2 unit. The values for σ^C and σ^A are given in Tables III and IV.

Z_I	σ^C	σ^A	σ^I	σ^R
16	2.0 (-5)	0	2.0 (-5)	1.3 (-5)
14	8.1 (-5)	7.0 (-5)	1.5 (-4)	1.9 (-5)
8	3.1 (-4)	3.5 (-5)	3.5 (-4)	2.4 (-5)
6	2.6 (-3)	8.3 (-3)	1.1 (-2)	3.4 (-5)
0	9.1 (-2)	7.5 (-3)	9.9 (-2)	1.1 (-4)
0'	1.0 (-1)	7.5 (-3)	1.1 (-1)	1.1 (-4)

Also included in Table V is the radiation emission cross section σ^R at 10 keV energy. The estimate of σ^R is uncertain mainly because of the poor accuracy in the fluorescence yield Y_α for higher shells. To be specific, we have used in our estimates $Y_K \cong 0.16$, $Y_L \cong 0.002$, and $Y_M \cong 0.0003$ for the K -, L -, and M -shell vacancies, respectively. (Y_M is less reliable and may be overestimated.)

Finally, the calculated total ionization cross section σ^I is compared with the experimental data¹⁰ in Table VI for E_k in the range $1 \leq E_k \leq 10$ keV. In view of the approximations involved, the agreement is reasonable, although the present calculation gives consistently lower cross sections than some of the earlier estimates. The previous theoretical results obtained by McGuire¹¹ and Omidvar¹² are also included for comparison. In σ^I , the adjustment of the threshold cutoff e_c for M_C substantially improves the result.

As the method used above for the argon ion can also be applied to other atomic systems with very little modification, we have studied the neutral Ne and O atoms interacting with the high-energy electrons. The transition probabilities for these

TABLE VI. The energy dependence of σ^C , σ^A , and σ^I , at $E_k = 1, 5$, and 10 keV. The cross sections are given in the πa_0^2 unit. The experimental values are given by σ_{exp}^I for the neutral argon target. MG is from Ref. 11, OKS is from Ref. 12. The experimental values are from Refs. 13–15. σ'^I is obtained with $e_c = -0.06$ Ry.

E_k (keV)	1	5	10
σ^C	0.62	0.17	0.091
σ^A	0.04	0.013	0.008
σ^I	0.66	0.18	0.10
σ'^I	0.74	0.20	0.11
σ^I (MG)	0.97	0.24	0.13
σ^I (OKS)	1.4	0.40	0.23
σ^I (expt)	0.8–1.2	0.22	0.12

cases are given in Table VII; they are then used to estimate σ^I . For both Ne and O, the M_C for the $2p-d$ transition is not affected by the adjustment of the cutoff e_c , mainly because of the already small values for M_B ; this was not the case with the neutral argon atom where M_B for the $3p-d$ transition was comparable to M_C . The resulting σ^I and σ^A are summarized in Table VIII, and compared with the available experimental^{13–19} and theoretical^{11,12,20} results. First of all, we note that σ^A is much smaller than σ^C , and the main contribution again comes from the $2p-d$ transition. (The σ^A contribution to the impact ionization becomes more important as Z_C increases.) Secondly, the multiplicity factor Z_α in the cross-section formula has to be chosen differently for Ne and for O; as the $2p$ subshell is filled in Ne, we chose $Z_{2p} = 6$, while for O we have $Z_{2p} = 4$. This difference in Z_{2p} is important, and the agreement with other results is quite satisfactory.

V. DISCUSSION

In this paper we have made two improvements in the calculation of the ionization cross section.

TABLE VII. Radial part of the dipole transition probabilities for the neutral Ne ($Z_C = 10$, $Z_I = 0$) and the neutral O ($Z_C = 8$, $Z_I = 0$). The details of the quantities listed here are the same as in Table II. The parameter values for the potential used are $d = 0.558$, $H = 1.512$ for Ne and $d = 0.735$, $H = 1.771$ for the O target, as given in Ref. 3.

Z_C	nl	\pm	e_{nl}	S	M_A	M_B	M_C	e_b	M_D	M_E
10	1s	p	61.47	0.879	0.034	0.016	0.018	1.2	0.001	0.019
	2s	p	3.17	0.876	1.03	0.76	0.27	1.2	0.52	0.79
	2p	s	1.62	0.880	1.23	1.21	0.02	2.0	0.81	0.82
	2p	d	1.62	0.880	1.23	0.04	1.19	a	0.04	1.23
8	1s	p	38.31	0.878	0.054	0.025	0.029	0.9	0.002	0.031
	2s	p	2.16	0.890	1.66	1.31	0.35	0.9	0.88	1.23
	2p	s	1.16	0.906	2.02	2.01	0.01	1.5	1.38	1.39
	2p	d	1.16	0.906	2.02	0.22	1.80	a	0.22	2.02

TABLE VIII. Total ionization cross sections for the neutral Ne and O targets by electron impact at the incident energy $E_k = 1, 5,$ and 10 keV. MG is from Ref. 11, OKS from Ref. 12, P from Ref. 20, and σ^I denotes the result of the present calculation. The experimental values are those of Refs. 13–19. There exists a considerable spread in the experimental as well as the theoretical values.

Z_C	Ref.	1 keV	5 keV	10 keV
10	σ^C	0.47	0.12	0.070
	σ^A	0.001	0.0004	0.0002
	σ^I	0.47	0.12	0.070
	MG	0.40	0.11	0.065
	OKS	0.45	0.13	0.075
	P	0.50	0.15	0.087
	expt	0.35–0.45	0.10<	0.06<
8	σ^C	0.52	0.14	0.075
	σ^A	0.002	0.0007	0.0004
	σ^I	0.52	0.14	0.075
	MG	0.45	0.12	0.07
	OKS	0.63	0.16	0.09
	expt	0.6–0.9	0.15–0.25	0.08–0.14

Firstly, the single-particle model for the many-electron target system has been improved,³ within the context of the original program.¹ This refinement does not seem to change the over-all qualitative conclusion obtained earlier¹ that σ^C dominates for low Z_C and σ^A at high Z_C , but the improvement is significant in terms of the reliability and accuracy. Secondly, the cross section σ^A depends rather sensitively on the cutoff

parameter e_b , which appears in Λ_D and Λ_E , while σ^C can sometimes be quite sensitive to the cutoff limit e_c (as in the neutral Ar case). Thus an accurate determination of e_c is important for cases with $Z_C \lesssim 30$ where σ^C dominates, and e_b for $Z_C \gtrsim 30$ where σ^A becomes larger. Our study of the hydrogenic system clarifies this problem of e_b and e_c , but fails to provide a more reliable procedure.

There are several additional points in our theoretical procedure which should be improved upon:

(i) The distortion of the wave function for the continuum electron in the initial and final states has been completely neglected here. This is justified for the incident energies higher than 1 keV and with Z_I small.^{12,23} This effect seems to reduce the cross section somewhat.

(ii) The contribution from the higher multipole transitions in (2.1) has been neglected; this should raise the cross section significantly.

(iii) Although the average excitation energy Δ appears in the cross section only logarithmically, a more systematic evaluation of Δ would be desirable, perhaps along the line suggested in Ref. 1.

ACKNOWLEDGMENTS

The author would like to thank Professor K. M. Watson for originally suggesting the problem and much early collaboration and Dr. K. Omidvar of NASA for a helpful discussion on the problem of the momentum-transfer cutoff in the cross-section formula. The computational part of the work reported here has been carried out at the University of Connecticut Computer Center, which is supported in part by a NSF grant.

¹Y. Hahn and K. M. Watson, Phys. Rev. A **7**, 491 (1973).

²A. E. S. Green, D. L. Sellin, and A. S. Zachor, Phys. Rev. **184**, 1 (1969).

³P. P. Szydlik and A. E. S. Green, Phys. Rev. A **9**, 1885 (1974).

⁴Y. Hahn and K. M. Watson, Phys. Rev. A **6**, 548 (1972).

⁵W. Bambynek, B. Craseman, F. W. Fink, H. U. Freund, H. Mark, C. D. Swift, R. E. Price, and P. V. Rao, Rev. Mod. Phys. **44**, 716 (1972).

⁶N. F. Mott and H. S. W. Massey, *The Theory of Atomic Collisions* (Oxford U. P., London 1965), Chap. 16.

⁷M. L. Goldberger and K. M. Watson, *Collision Theory* (Wiley, New York, 1964), Chap. 8.

⁸H. A. Bethe and R. W. Jackiw, *Intermediate Quantum Mechanics* (Benjamin, New York, 1968); see also M. Inokuti, Rev. Mod. Phys. **43**, 297 (1971); B. L. Moiseiwitsch and S. J. Smith, *ibid.* **40**, 238 (1968); M. R. H. Rudge, *ibid.* **40**, 564 (1968).

⁹H. A. Bethe and E. Z. Salpeter, in *Handbuch der Physik*, edited by S. Flügge (Springer, Berlin, 1957), Vol. 35.

¹⁰L. J. Kieffer and G. H. Dunn, Rev. Mod. Phys. **38**, 1 (1966).

¹¹E. J. McGuire, Phys. Rev. A **3**, 267 (1971).

¹²K. Omidvar, H. L. Kyle, and E. C. Sullivan, Phys. Rev. A **5**, 1174 (1972).

¹³P. T. Smith, Phys. Rev. **36**, 1293 (1930).

¹⁴D. Rapp and Englander-Golden, J. Chem. Phys. **43**, 1464 (1965).

¹⁵B. L. Schram, F. J. de Heer, M. J. van der Wiel, and J. Kistemaker, Physica (Utr.) **31**, 94 (1964).

¹⁶A. Goudin and R. Hagemann, J. Chem. Phys. **64**, 1209 (1967).

¹⁷W. L. Fite and R. T. Brackmann, Phys. Rev. **113**, 815 (1959).

¹⁸E. W. Rothe, L. L. Marino, R. H. Neynaber, and S. M. Trujillo, Phys. Rev. **125**, 582 (1962).

¹⁹A. Boksenberg, thesis (University of London, 1961).

²⁰G. Peach (unpublished).

²¹C. E. Moore, *Atomic Energy Levels* (U. S. Nat. Bur. Stand., U. S. GPO, Washington, D.C., 1958).

²²Von W. Finkelberg and W. Humbach, Naturwissenschaften **42**, 35 (1955).

²³S. J. Wallace, R. A. Berg, and A. E. S. Green, Phys. Rev. A **7**, 1616 (1973).